AGU PUBLICATIONS

JGR

Journal of Geophysical Research: Atmospheres

RESEARCH ARTICLE

10.1002/2013JD020063

Key Points:

- Elevated temperature inversion produced two bright bands simultaneously
- Rapid evolution of freezing levels in response to approaching warm front
- Identification of double bright bands important for estimating rainfall

Correspondence to:
A. E. Emory,
amber.emory@nasa.gov

Citation:
Emory, A. E., B. Demoz, K. Vermeesch, and M. Hicks (2014), Double bright band observations with high-resolution vertically pointing radar, lidar, and profilers, *J. Geophys. Res. Atmos.*, *119*, 8201–8211, doi:10.1002/2013JD020063.

Received 19 APR 2013
Accepted 19 MAY 2014
Accepted article online 23 MAY 2014
Published online 8 JUL 2014

Double bright band observations with high-resolution vertically pointing radar, lidar, and profilers

Amber E. Emory[1], Belay Demoz[2], Kevin Vermeesch[3], and Micheal Hicks[4]

[1]NASA Goddard Space Flight Center, Greenbelt, Maryland, USA, [2]Department of Physics and Astronomy, Howard University, Washington, District of Columbia, USA, [3]Science Systems and Applications, Inc., Lanham, Maryland, USA, [4]National Weather Service, Sterling, Virginia, USA

Abstract On 11 May 2010, an elevated temperature inversion associated with an approaching warm front produced two melting layers simultaneously, which resulted in two distinct bright bands as viewed from the ER-2 Doppler radar system, a vertically pointing, coherent X band radar located in Greenbelt, MD. Due to the high temporal resolution of this radar system, an increase in altitude of the melting layer of approximately 1.2 km in the time span of 4 min was captured. The double bright band feature remained evident for approximately 17 min, until the lower atmosphere warmed enough to dissipate the lower melting layer. This case shows the relatively rapid evolution of freezing levels in response to an advancing warm front over a 2 h time period and the descent of an elevated warm air mass with time. Although observations of double bright bands are somewhat rare, the ability to identify this phenomenon is important for rainfall estimation from spaceborne sensors because algorithms employing the restriction of a radar bright band to a constant height, especially when sampling across frontal systems, will limit the ability to accurately estimate rainfall.

1. Introduction and Background

Observations of radar bright bands, which are primarily the result of a rapid increase in the dielectric constant from the change of frozen ice aggregates to liquid water at the top of the melting layer in addition to an increase in the fall speed of raindrops once the melting process is complete [*Battan,* 1973], have occurred for a long time [*Marshall et al.*, 1947; *Cunningham*, 1947]. Melting alters both the density and dielectric factor of hydrometeors as they pass through the melting layer, enhancing radar reflectivity returns due to the presence of liquid water around a still frozen interior [*Fabry and Zawadzki*, 1995; *White et al.*, 2002; *Giangrande,* 2007]. Beneath the melting layer, the decrease in reflectivity is due to hydrometeors fully melting and forming smaller particle sizes and terminal velocity increasing, which removes them from the radar sampling volume at a faster rate. Several previous papers have discussed multiple bright bands using vertically pointing X band radars [*Fabry et al.*, 1992; *Fabry and Zawadzki*, 1995], S band profilers [*Martner et al.*, 2007], and polarimetric radars [*Ikeda et al.*, 2005]; however, this is the first instance of a double bright band sampled using a coherent X band radar at high temporal resolution (0.5 s) to measure reflectivity, vertical velocity, and spectrum width associated with these phenomena. The high temporal and spatial resolution of ER-2 Doppler (EDOP), combined with other observations, reveals a detailed time evolution of double bright bands and the meteorological causes of this evolution.

In stratiform precipitation, vertical reflectivity varies as a function of height and changes rapidly around the melting layer. The bright band appears as a horizontal narrow layer of enhanced reflectivity about 200 to 400 m below the 0°C isotherm [*Stewart et al.*, 1984; *Willis and Heymsfield*, 1989; *Martner et al.*, 1993, 2007] and can have a depth of 200 to 500 m [*Fabry et al.*, 1992]. The bright band thickness also increases with precipitation intensity, which can be explained by the increased aggregation of larger snowflakes that take more time to melt. Vertical Doppler velocity profiles reveal a marked increase in the magnitude of downward velocities and broadened spectra below the melting layer, where slowly falling snowflakes/aggregates melt and become rapidly falling liquid raindrops [*Fabry et al.*, 1992]. The height of the melting layer can vary rapidly, particularly in the case of precipitation accompanying an approaching front. In order to capture these rapid changes, radar with high spatial (on the order of 20 m) and temporal resolution (on the order of 1 s) is necessary [*Fabry et al.*, 1992].

Normally, a vertical temperature profile through the atmosphere contains only one melting level, which results in a single bright band. However, when warm air arrives aloft before it reaches the surface, as with an approaching warm front, there may be two or more altitudes with 0°C isotherms with corresponding bright

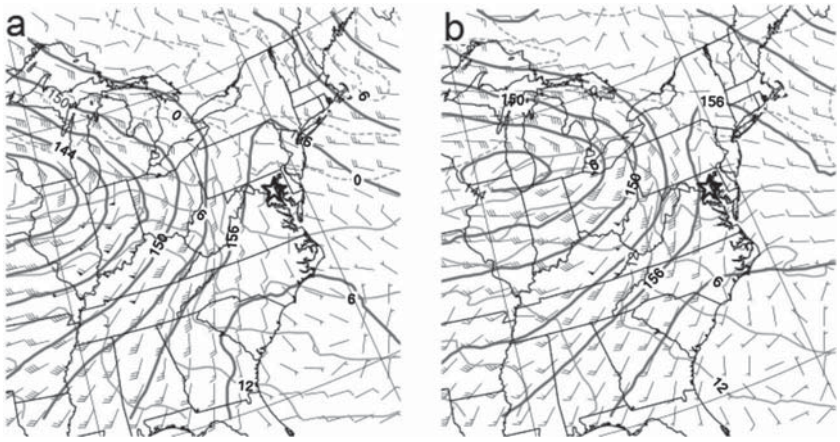

Figure 1. An 850 hPa map of the mid-Atlantic region at (a) 1200 UTC and (b) 1800 UTC on 11 May 2010. The wind barbs are in knots, the heavy dark gray lines are 850 hPa height contours (in dam), and the thin gray lines are the 850 hPa temperature contours (in °C). The solid lines are for temperatures above freezing, and the dashed lines are at or below freezing. The location of instruments at the Howard University Beltsville Research Center and NASA Goddard are indicated by a black star over the Washington, DC metropolitan area.

bands beneath each melting layer. Multiple bright bands can occur when a shallow layer with a temperature above 0°C overlays another layer of freezing temperatures. In this region, snowflakes begin to melt, resulting in a bright band at higher altitude, but fail to melt completely, refreeze in the cold layer, and melt again further down. Multiple bright bands are uncommon but have been seen previously [*Plank et al.*, 1955; *Fabry and Zawadzki*, 1995; *Ikeda et al.*, 2005; *Martner et al.*, 2007]. In the survey completed by *Fabry and Zawadzki* [1995], less than 2% of their 600 h of data collected represented double or multiple bright band cases. In addition, *Fabry and Zawadzki* [1995] noted that multiple bright bands were most common during the transition between summer and winter when strong fronts that cause temperature inversions a few kilometers above the surface moved through their region (Montreal, Quebec).

Bright bands represent a challenge for radar-based rainfall rate estimation because the enhanced reflectivities give an exaggerated impression of rainfall occurring at the surface. For example, *Fabry et al.* [1992] showed that when only the bright band is sampled, the rainfall could be overestimated by a factor of 5 at near range. However, rainfall is underestimated as more frozen ice crystals fill the beam. This is caused by the fact that, at microwave frequencies, the dielectric factor of ice (0.18) is much less than that of pure liquid water (0.93). In addition, the change of density from ice to liquid water results in a difference of approximately 6.5 dB in the reflectivity of a liquid raindrop when compared to a sphere of ice at the same mass [*Pruppacher and Klett*, 1978; *Fabry and Zawadzki*, 1995]. At centimeter and longer microwave wavelengths, the enhanced scattering of the bright band results in enhanced reflectivity and increased signal extinction [*Fabry and Zawadzki*, 1995]. Knowing the level of attenuation caused by the melting layer is crucial to properly estimate rainfall using short-wavelength spaceborne radars, such as the Tropical Rainfall Measurement Mission (TRMM) and the Global Precipitation Measurement (GPM) mission [*Kummerow et al.*, 1998; *Battaglia et al.*, 2006].

In this paper, we report on a multi-instrument data set collected during a double bright band event over the Washington, DC metropolitan region on 11 May 2010. Synoptic conditions for the case are discussed in section 2, a brief description of the instruments and data used is in section 3, and a discussion of the observations and the EDOP radar is given in section 4. Synthesis and discussion of the results is given in section 5.

2. Synoptic Conditions

On the morning of 11 May 2010, the axis of a deamplifying 500 hPa ridge that was transitioning to zonal flow with a weakening low-pressure system located over the southern Great Lakes was located near the mid-Atlantic region. A surface high pressure was located off the mid-Atlantic coast. A 500 hPa shortwave trough approaching from the southwest reached the mid-Atlantic region at approximately 1200 UTC and marked the leading edge of an area of 700 hPa moisture convergence followed by strengthening 850 hPa warm air advection. Figure 1 shows that between 1200 and 1800 UTC, the 850 hPa 0°C isotherm, originally located in

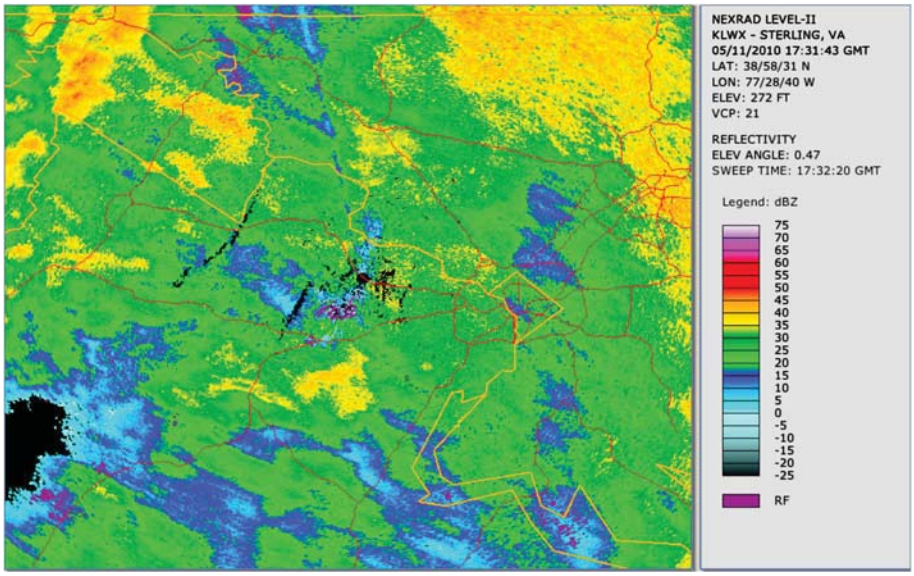

Figure 2. Level-II reflectivity from the 1731 UTC volume from the Sterling, VA (KLWX) radar shows widespread stratiform rain showers associated with the double bright band case. State borders are mustard yellow, and major roadways are red.

south central Pennsylvania, moved into southern Maryland during the time of the double bright band occurrence, while the 850 hPa temperature gradient strengthened over Virginia. By 1800 UTC, the surface low pressure was located near southern Lake Michigan and the surface warm front had moved northward into the vicinity of Washington, DC, accompanied by bands of light stratiform rain showers as shown in Figure 2.

3. Instrumentation

The Howard University Beltsville Research Campus (HUBRC) is located approximately 19 km northeast of downtown Washington, DC, on 25 km in suburban Maryland. The campus is in a rural setting and contains minimal development with no more than 5% of the land area occupied by building structures, making it an ideal environment for studying a range of surface-atmosphere interaction processes. The instrumentation available at the site includes several spectral and broadband radiometers, GPS-based water vapor, microwave profilers, total sky imager, radiosondes, Raman lidar for aerosol and water vapor profiling, a ceilometer, 32 m flux and meteorological tower, rain gauges, and NO_x, ozone, and CO analyzers and particle samplers. The HUBRC site is also located 11 km from the NASA Goddard Space Flight Center (GSFC) in Greenbelt, MD, where a vertically pointing X band radar sampled the double bright band event. A brief summary of the main instruments used in the discussion is given below.

3.1. EDOP

EDOP is a vertically pointing radar with a 0.31 m diameter offset parabolic reflector antenna with an 8° beamwidth and 37.5 m range resolution. A pulse repetition frequency of 4400 Hz yields a Nyquist velocity of 34.4 m s^{-1} and a maximum unambiguous range of 34.1 km [*Heymsfield et al.*, 1996], although the signal suffers significant attenuation above 10 km when transmitting through heavy precipitation (>60 dBZ) from the surface. At the time the measurements for the 11 May 2010 case were collected, EDOP had one vertically pointing beam. An upgrade to the system is currently underway to add in a second 30° off zenith-pointing beam with polarimetric capability. The S band profilers used to measure vertical profiles of reflectivity and vertical velocity in *Martner et al.* [2007] had comparable spatial resolution (60 m gate spacing) but far less temporal resolution (30 s) than recommended for capturing rapid changes in the height of the melting layer. EDOP [*Caylor et al.*, 1994; *Heymsfield et al.*, 1996] is a coherent X band (9.6 GHz/3.123 cm) frequency radar that was built in 1994 and flown in multiple field campaigns, such as the Convection and Moisture Experiments from 1993 to 2001, the Cirrus Regional Study of Tropical Anvils and Cirrus Layers in 2002, and the Tropical Cloud Systems and Processes field campaign in 2005. EDOP worked consistently as a ground-based vertically pointing radar with an antenna housed at NASA GSFC from 2007 until 2011. This radar was operational during the case

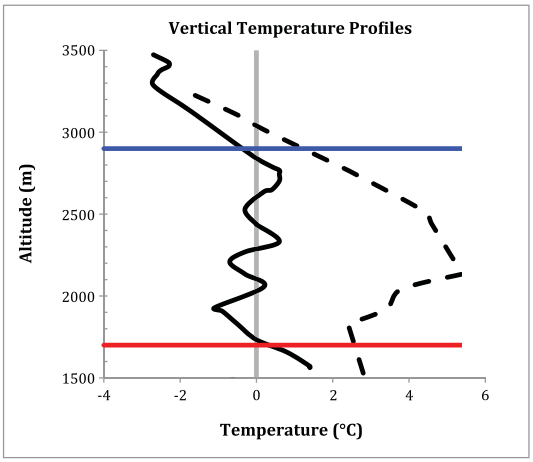

Figure 3. Vertical temperature profiles from 1200 UTC 11 May 2010 and 0000 UTC 12 May 2010 soundings taken in Sterling, VA, with bright band altitudes determined from EDOP overlaid. The solid black line is the vertical temperature profile from the 1200 UTC 11 May 2010 sounding, the dashed black line is the vertical temperature profile from the 0000 UTC 12 May 2010 sounding, the red line is the height of the first bright band that appeared at 1.7 km, the blue line is the height of the second bright band that appeared at 2.9 km with the arrival of the warm front aloft before reaching the surface, and the vertical gray line marks the melting level.

study of interest here and measured the evolution of the reflectivity, vertical velocity structure, and spectrum width with 0.5 s temporal and 37.5 m spatial resolution, which allows a detailed evolution of the double bright band feature of this case to be captured.

3.2. Microwave Radiometer Profiler

The microwave profiler is a Radiometric MP-3000A (see http://radiometrics.com for details and an extensive reference list) that retrieves temperature, water vapor, and cloud water at 2 min time intervals in nonprecipitating conditions by measuring microwave radiance as brightness temperatures for 47 vertical levels—11 levels from the ground up to 1 km with 100 m vertical resolution and 36 levels from 1 km to 10 km with 250 m vertical resolution. It uses 21 frequencies between 22.0 and 30.0 GHz for water vapor sensing (K band) and 14 frequencies between 51.3 and 58.8 GHz for temperature sensing (V band). The K band frequencies are near the 22 GHz water vapor emission line, and the V band frequencies are near the 60 GHz oxygen emission line. The mixing ratio of oxygen is constant with height, so emissions variations in the V band are a function of temperature. Probing the range of V band frequencies allows emissions from different heights to be sensed, thus creating a temperature profile. Water vapor emissions from K band frequencies are proportional to water vapor density and height (due to pressure broadening of the line shape), which allows a profile of water vapor density to be obtained.

3.3. The 915 MHz Profiler and Ceilometer

At the Howard University Beltsville site, the Maryland Department of the Environment (MDE) has a 915 MHz DeTect RAPTOR DBS-BL/LAP-3000 radar wind profiler that operates by transmitting electromagnetic energy vertically and in north-south and west-east vertical planes. The Doppler frequency shift of the backscattered energy retrieved from this transmission is then used to measure wind speed and direction. In addition, the MDE wind profiler and radio acoustic sounding system (RASS) combination measures wind profiles from the surface to approximately 4 km, depending on atmospheric aerosol loading, and virtual temperature profiles to approximately 2.5 km. The RASS-profiler combination is used to measure the virtual temperature profile in the lowest 100 to 200 m of the atmosphere. The technique relies on a matching of the transmitted acoustic signal wavelength to half wavelength of radar signals where the speed of the sound wave is determined. The propagation speed of the acoustic wave is proportional to the square root of the virtual temperature [*Angevine et al.*, 1998].

The ceilometer used in this study is a Vaisala CT25K with a vertical range of 7 km and uses an eye-safe, class 1-pulsed Indium Gallium Arsenide diode laser at a wavelength of 905 nm with a 1.6 μJ pulse at 5 kHz.

4. Results

4.1. Radiosondes and Surface Measurements at HUBRC

The vertical temperature profiles in Figure 3 show the advancing warm front below 3.1 km altitude. Elevated temperature inversions in the 1200 UTC 11 May 2010 and 0000 UTC 12 May 2010 Sterling, VA soundings and the advection of warm air aloft preceded the passage of the front at the surface. The two soundings also show a significant warming of up to 6°C in the layer between 1.5 and 3.1 km in the 12 h time period. This layer was capped by a fast-moving westerly jet and was characterized by several layers of opposite lapse rates in the 1200 UTC profile that could loosely be approximated cold-warm cycles.

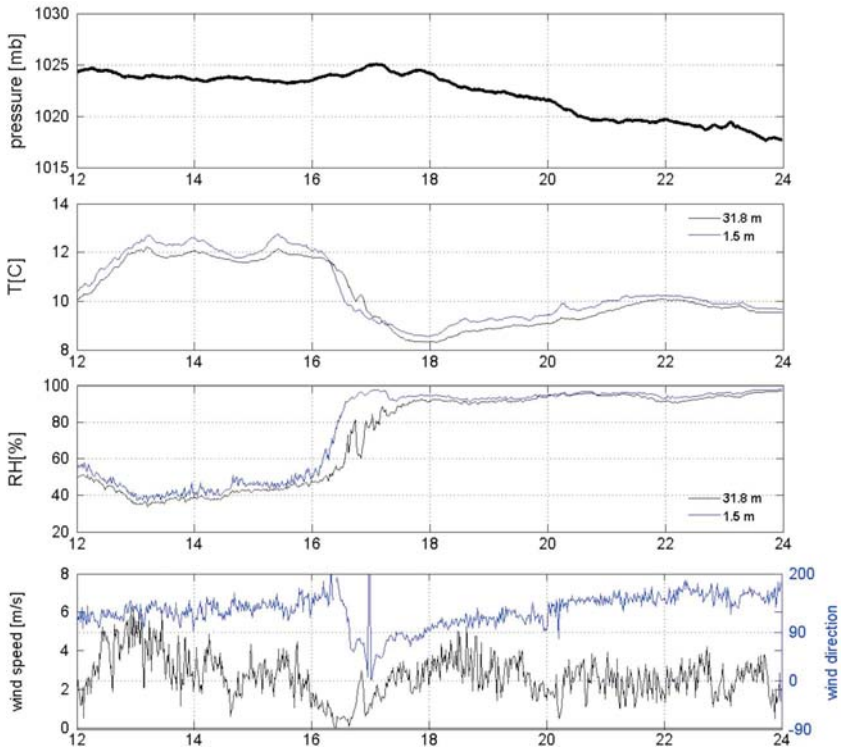

Figure 4. Time series (1200–2400 UTC on 11 May 2010) of flux tower pressure, temperature, relative humidity, and wind speed and direction at 1.5 m and 31.8 m altitude at the Howard University Beltsville site, which is located approximately 7.75 km north of the location where the EDOP radar is located at NASA Goddard Space Flight Center.

Figure 4 shows a surface pressure decrease of 7 mb from 1200 UTC on 11 May 2010 to 0000 UTC on 12 May 2010, accompanied by a 4°C temperature drop and an abrupt increase in relative humidity with the initiation of stratiform rain after 1630 UTC. The surface pressure increased slightly after the stratiform rain reached the Howard University Beltsville site associated with the arrival of the cold pool due to evaporational cooling, which can also be seen with the sharp drop in temperature after 1600 UTC. The wind direction shift shown just after 1700 UTC in Figure 4 (bottom) gives the best indication of the time when the warm air mass arrived at the surface.

4.2. EDOP and Vertical Profiles of Reflectivity

For this case, the colocation of velocities with reflectivity gives insight into the characteristics of hydrometeors over the evolution of the double bright band feature. For vertically pointing radar, the estimation of mean Doppler velocity is the updraft velocity minus the particle terminal fall velocity [*Pruppacher and Klett*, 1978]. Above the melting layer, snow fell slowly (0.5 to 2 m s^{-1}) relative to liquid hydrometeors below the bright band shown in Figure 5, which is comparable to those in previous studies such as *Fabry and Zawadzki* [1995]. Below the bright band, complete melting occurred where fall speeds reached values greater than approximately 5 m s^{-1}, which is a typical value for small raindrops. Interestingly, with the start of the double bright band at approximately 1719 UTC on 11 May 2010, downward vertical velocity speeds failed to increase to 5 m s^{-1} below the elevated melting layer, which suggests that while some melting at the surface of frozen aggregates may have occurred to produce the first bright band at 2.9 km, refreezing likely occurred quick enough to keep hydrometeors from obtaining falling speeds more closely associated with liquid raindrops. The changes in spectrum width closely mimic the changes seen with the vertical velocities. The increase in spectrum width from approximately 1 m/s to 4 m/s in the layer between the two melting layers after 1735 UTC also shows the transition from frozen or partially frozen aggregates to liquid drops.

As the warm front approached during the morning hours of 11 May 2010, an elevated melting layer formed above a lower, preexisting melting layer closer to the surface. The vertical profiles of reflectivity at two separate times before (1702 UTC) and after (1744 UTC) the passage of the warm front at the surface are

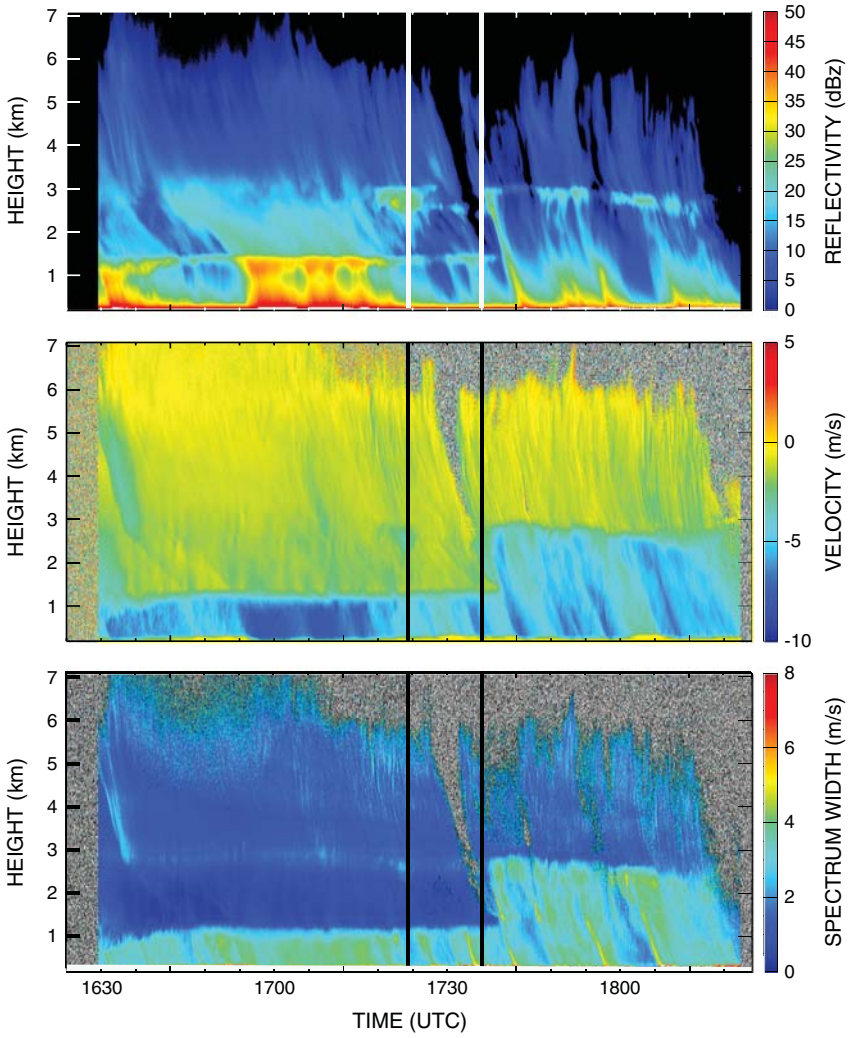

Figure 5. EDOP (top) reflectivity, (middle) vertical velocity, and (bottom) spectrum width during the warm front passage on 11 May 2010. Vertical lines mark the start (1719 UTC) and end (1735 UTC) of the double bright band feature.

shown in Figure 6. At 1702 UTC, the main bright band was located at approximately 1.5 km altitude, although a secondary localized reflectivity maximum existed at 2.5 km altitude, which can be expected as the warm front advanced further aloft before reaching the surface. However, by 1744 UTC, the primary bright band ascended to 2.9 km altitude following the surface warm front passage and warming of the entire layer below 2.9 km altitude to above 0°C. Similar to what *Ikeda et al.* [2005] observed, it appears that continued warming of the lower atmosphere eventually erased the lower melting layer. Based on the Doppler vertical velocities, hydrometeors that melted below the higher bright band never refroze and continued to fall to the surface as liquid precipitation.

4.3. The 915 MHz Profiler and Ceilometer

The warming associated with the passage of the surface front at low levels is captured by the microwave profiles shown in Figure 7. The dashed line in Figure 7a shows the microwave radiometer (MWR) profiler-measured 0°C contour and the subsequent lift of the lower warm layer starting at approximately 1630 UTC with the 0°C temperature line lifting from approximately 1.3 to more than 2.2 km altitude. Figure 7b is a zoomed-in plot in the lowest 1 km above the surface and shows the convergence along the front at 1630 UTC followed in time by low-level cold air topped by a relatively warm air layer and followed by a colder air mass again up to about 3.2 km altitude. Figure 7c shows temperature and backscatter profiles measured with the MWR and ceilometer, respectively. The two levels of dark band (identified as "DB" in the figure) as measured by the

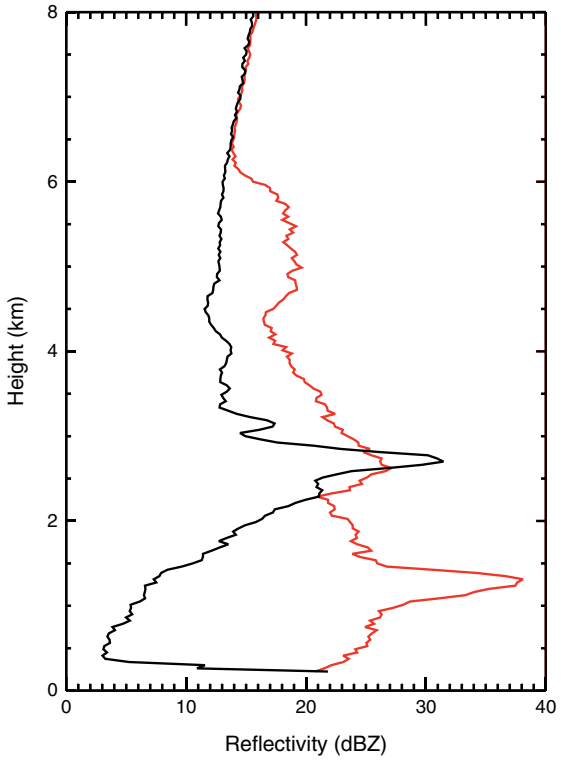

Figure 6. Vertical reflectivity profiles for EDOP at 1702 UTC (red) and 1744 UTC (black) on 11 May 2010. The increase in the altitude of the primary bright band is due to the passage of a warm front.

ceilometer backscatter are a manifestation of the radar bright band at the shorter visible wavelength. The difference in altitude of the 0°C isotherm and the dark band is in agreement with previous studies [see *DiGirolamo et al*., 2003].

Similarly, Figure 8 shows a time series of unsmoothed measurements of surface pressure, cloud base temperature, and freezing height. For the freezing height, the first peak is located at an altitude of 2.25 km and started at approximately 1632 UTC with the arrival of the warm front aloft, which corresponds with the drop in surface pressure and the increase in cloud base temperature from 270 to 277. The deepening of the warm layer and lifting of the freezing height corresponds well with the time that the double bright band was captured with the EDOP radar. However, note that the MWR is a passive remote sensing instrument that has low vertical resolution and hence is not able to reveal sharp gradients or double bright band structures.

Figure 9 shows that the dark band in the ceilometer data is just above 1 km altitude beginning at 1600 UTC, shortly before precipitation reached the surface. The decreased backscatter in the dark band is due to the smaller cross section of raindrops that resulted from the sudden collapse

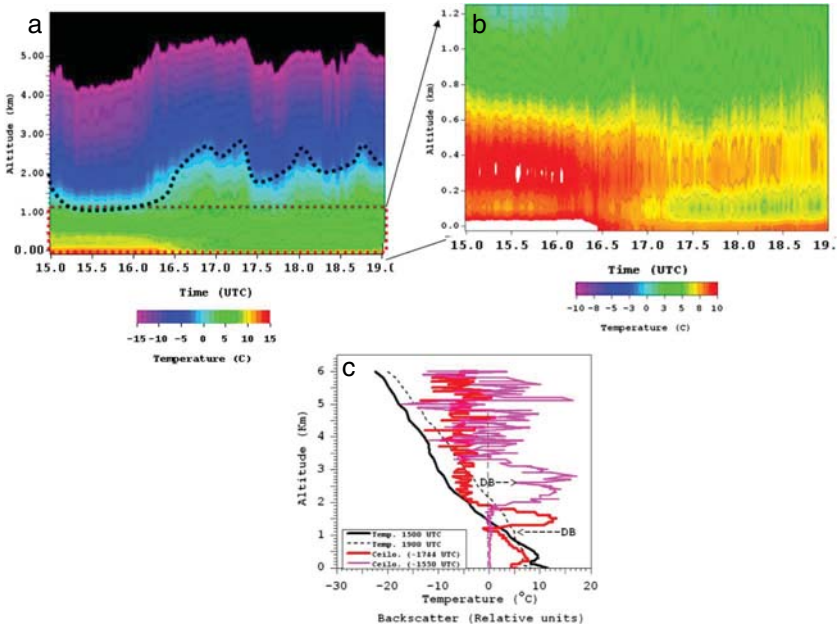

Figure 7. (a) An expanded plot of the MWR temperature between 1500 and 1900 UTC reveals deepening of the warm layer and the lifting of the 0°C layer contour starting at 1630 UTC. (b) A zoomed-in plot of the lowest kilometer shows a convergence region at 1630 UTC followed by a cold-warm-cold stratification. (c) Temperature profiles measured with the 915 MHz profiler and backscatter profiles from the ceilometer. The two levels of dark band (identified as "DB") as measured by the ceilometer backscatter are a manifestation of the radar bright band at the shorter visible wavelength.

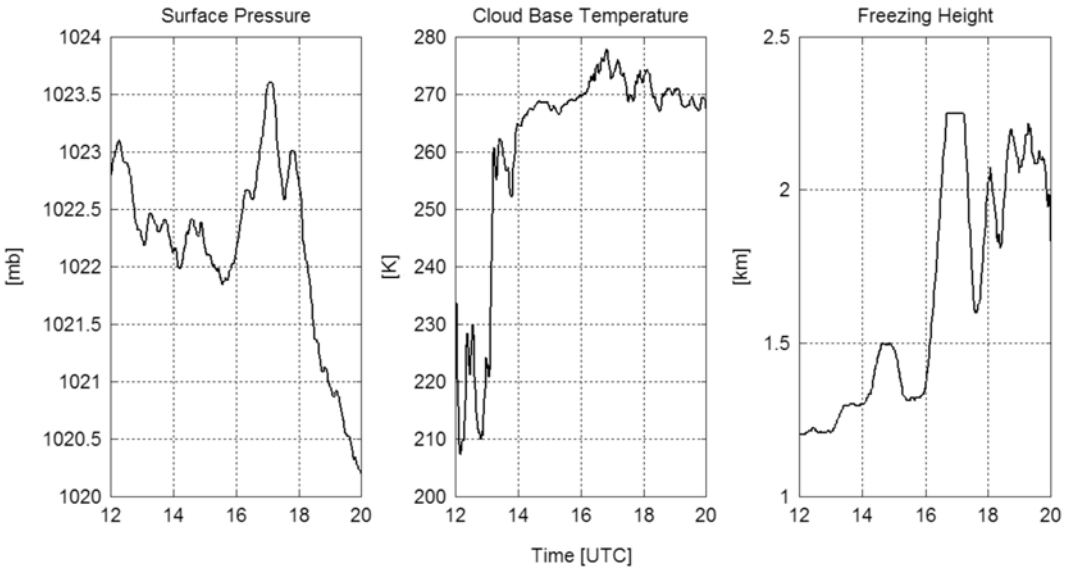

Figure 8. (left) Surface pressure, (middle) cloud base temperature, and (right) freezing height for the south pointing beam of the Howard University Beltsville site microwave radiometer profiler.

of melted snow flakes at this level and the faster falling speed of raindrops compared to snowflakes that result in a decrease of cloud particle concentration [*Sassen and Chen*, 1995]. The increase of backscatter below the dark band is due to the increased scattering from the spherical particles that could possibly include ice cores leading to specular reflection [*Sassen and Chen*, 1995; *Demoz et al.*, 1998; *Di Girolamo et al.*, 2003]. The height of the dark band is approximately 300 m below the freezing level indicated at 1.7 km in Figure 3, in agreement with *DiGirolamo et al.* [2003]. The 1200 UTC 11 May 2010 sounding indicates that there was a dry layer with 45% relative humidity (RH) just below 1.5 km. The RH at the freezing level of the 1200 KIAD sounding was approximately 70% (not shown). *Mitra et al.* [1990] found that the height of snowflake melting is lowered approximately 100 m for each 10% of subsaturation due to the cooling effects of sublimation. The estimate of 70% RH puts the height of the dark band in agreement with the ambient temperature and humidity profiles.

The dark band continued at the same altitude from 1600 UTC to past 1900 UTC. Ceilometer backscatter data could not be used to ascertain if there was or was not a dark band above approximately 1.7 km because the signal was attenuated above that height, due to optically thick (precipitating) clouds. However, a dark

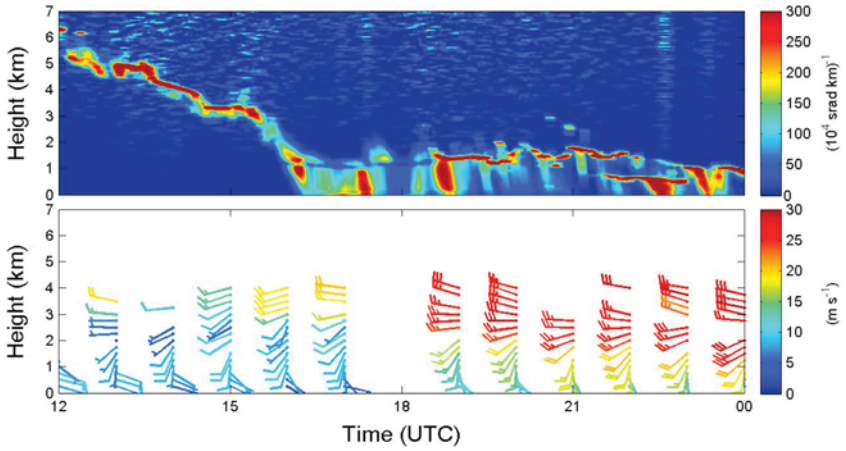

Figure 9. Time-height plots of data for 11 May 2010. (top) Vaisala CT25K ceilometer freezing height backscatter and (bottom) wind profiler speed and direction. The ceilometer and wind profiler are located at the Howard University Beltsville Research. The ceilometer is averaged for 1 min temporally and 40 m vertically.

band was observed in the ceilometer data in the lowering clouds at approximately 1550 UTC and 2.7 km altitude, before any precipitation was observed (see Figure 7c). In addition, a temperature contour plot from the MWR profiler reveals that the 0°C contour line dramatically rose to higher altitudes with the passage of the warm front. Since the passive microwave temperature uses smoothed weighting functions to retrieve the temperature and does not do well in sharp temperature transitions, the 0°C contour could easily even be higher than what is shown. The presence of the 1 km dark band and the 3 km radar bright band form a crude boundary for the oscillating freezing level altitudes seen in the MWR data.

Wind profiler data in Figure 9 (bottom) show a region of southeasterly flow capped by southerly flow. The veering of winds in the vertical is another indication of warm air advection associated with the advancing warm air mass aloft from the south. This layer of southerly flow steadily lowered toward the surface from 1500 to 1900 UTC and is another indication of the layer warming, which eventually caused a higher, single bright band to develop at 2.9 km and refreezing of hydrometeors to fail to occur.

5. Discussion and Conclusions

On 11 May 2010, an elevated temperature inversion associated with an approaching warm front produced two separate melting layers simultaneously, which resulted in two distinct bright bands as viewed from the vertically pointing EDOP radar. Prior to the temperature inversion aloft, a single melting layer and bright band were located at approximately 1.7 km altitude. As the warm air mass advanced aloft, the appearance of a second freezing level occurred at 2.9 km altitude. A double bright band was evident from EDOP radar data for approximately 17 min, which corresponds well to double bright band measurements of 20 to 40 min with the S-Pol radar in *Ikeda et al.* [2005]. The descent of the front toward the ground resulted in warming of the lower atmosphere, which dissolved the lower freezing level at 1.7 km altitude and left only the upper bright band at 2.9 km altitude after 1735 UTC. The refreezing of hydrometeors between the two bright bands eventually ended once the lower atmosphere below 2.9 km warmed above 0°C. The end result left only light rain, which can be seen from the increased downward vertical velocities, in the near 3 km layer below the newly elevated melting layer after 1735 UTC.

Fabry and Zawadzki [1995] found that melting by itself is not a sufficient condition for the appearance of a radar bright band feature. They hypothesized that small vertical air velocities as well as a much lower fall speed of frozen precipitation above the melting layer versus the fall speed of fully melted raindrops are required for a bright band to be present. This can be seen in Figure 5, where velocity and radar reflectivity are colocated, as the area between the two melting levels warms and the lower bright band feature erodes, once the higher bright band at 2.9 km altitude became fully established the downward (negative) vertical velocities increased in magnitude.

The 1200 UTC 11 May 2010 sounding in Figure 3 is representative of the EDOP time series up to approximately 1735 UTC. At this time, the vertical temperature profile at 1200 UTC finally warmed above 0°C at 1.75 km altitude, just above the height of the bright band (1.7 km). In addition, the 1200 UTC sounding suggests that ahead of the front a warm layer of air is advancing aloft. Figure 3 shows a temperature inversion with temperatures straddling the 0°C isotherm in a layer nearly 1.5 km thick. This suggests that melting occurred inefficiently and might also explain the approximately 17 min of observed double bright band. The temperature profile suggests that only partial melting of falling snow aggregates occurred in the thin elevated warm layer and that refreezing occurred in the cold air beneath it. The refrozen hydrometeors then completely melted upon reaching the melting layer at 1.7 km. Melting often creates isothermal layers near 0°C, as was observed, and pressure perturbations, which can modify the kinematic structure of a storm [*Atlas et al.*, 1969; *Marwitz*, 1983, 1987]. In contrast, the 0000 UTC 12 May 2010 sounding was more representative of the EDOP time series after 1735 UTC. After warm air filled the lower atmosphere, the melting layer rose to 3.05 km altitude and the associated bright band occurred at 2.9 km. Since no part of the temperature profile below 3 km approached the freezing level again, this would explain the eventual disappearance of the bright band at 1.7 km.

Similar to *Fabry et al.* [1992], we found that the temperature increased to above 0.5°C followed by a refreezing of temperatures lowering to less than −1°C before the second melting layer was encountered (Figure 3). Figure 5 and the 1200 UTC sounding in Figure 3 both suggest that when the two separate melting levels were first observed, melting was inefficient in the upper layer as the particles partially refroze before passing through the second melting layer. Incomplete melting of frozen aggregates to liquid raindrops can also be

due to the thickness of the warm layer that hydrometeors pass through. Although it is a separate double bright band case, *Ikeda et al.* [2005] showed that between the two melting layers captured by S-Pol, which has a cross-polarization isolation of −35 dB, linear depolarization ratio values decreased only to −23.4 dB at 1.5 km altitude. This shows that the hydrometeors did not completely melt before refreezing and further supports, from a separate but synoptically similar case, that inefficient melting occurred within the first melting layer. Recent work by *Melnikov* [2013] shows that with polarimetric radars there are cases of low ρ_{hv} areas that may indicate the presence of localized wet aggregates above the melting layer. At the time when the measurements shown in this paper were obtained, EDOP was not a polarimetric radar. However, current upgrades to the system include a dual polarimetric beam that will point 30° off zenith to provide polarimetric variables to further investigate the appearance of wet aggregates above the melting level.

This case shows the relatively rapid evolution of freezing levels in response to an advancing warm front over a 2 h time period and the descent of the elevated warm front with time. The stable (inversion) layer associated with the warm layer aloft was located between 1.7 and 3.0 km in the 1200 UTC 11 May 2010 sounding (Figure 3). The next sounding shows considerable warming in that layer (up to +6°C in some areas). This suggests that a warm air layer aloft overlaid a cooler air mass. Thus, only a single freezing level existed close to the ground up to 1719 UTC. With the arrival of warm air aloft at 3.0 km associated with the inversion, the upper bright band appeared at 2.9 km, which is characteristic of the bright band to be located on the order of 100 m below the 0°C isotherm [*Stewart et al.*, 1984]. The leading edge of the warm air is depicted by hints of an elevated bright band at 1719 UTC and as the lower atmosphere warmed in time, the lower melting layer eroded.

These results show that the ability to identify bright band heights in real time is essential. Thus, the restriction of a radar bright band to a constant height, especially when sampling across frontal systems, will seriously limit the ability to accurately estimate rainfall. This case study has important implications regarding the number of double (or multiple) bright band cases that may occur in precipitation events associated with frontal passages and that spaceborne sensor algorithms should consider their presence when estimating rainfall rate. Furthermore, the case demonstrates the advantages that can be gained in understanding the dynamics and structure of precipitation systems when observed simultaneously with a multi-instrument suite.

Acknowledgments

The authors would like to thank Gerald Heymsfield, Lin Tian, and Everette Joseph for fruitful and informative discussions about this case. The authors would also like to thank Kevin Witt from the Sterling, VA NWS forecast office for help with the forecast discussion and the Maryland Department of the Environment for the 915 MHz profiler data. The instruments operated at the Howard University Beltsville site are funded by NASA under the University Research Centers (URC) and NOAA Center for Atmospheric Studies.

References

Angevine, W. M., A. W. Grimsdell, L. M. Hartten, and A. C. Delany (1998), The Flatland boundary layer experiments, *Bull. Am. Meteorol. Soc.*, *79*, 419–431.

Atlas, D., R. Tatehira, R. C. Srivastava, W. Marker, and R. E. Carbone (1969), Precipitation-induced mesoscale wind perturbations in the melting layer, *Q. J. R. Meteorol. Soc.*, *95*, 544–560.

Battaglia, A., M. O. Ajewole, and C. Simmer (2006), Evaluation of radar multiple-scattering effects from a GPM perspective. Part I: Model description and validation, *J. Appl. Meteorol. Climatol.*, *45*, 1634–1647.

Battan, L. J. (1973), *Radar Observations of the Atmosphere*, 279 pp., Univ. of Chicago Press, Chicago, Ill.

Caylor, I. J., G. M. Heymsfield, S. W. Bidwell, and S. Ameen (1994), NASA ER-2 Doppler radar reflectivity calibration for the CAMEX Project, NASA Technical Memorandum 104611.

Cunningham, R. M. (1947), A different explanation of the "bright line", *J. Meteorol.*, *4*, 163.

Demoz, B., D. Starr, K. Chan, and S. Bowen (1998), Wavelet analysis of dynamical processes in cirrus, *Geophys. Res. Lett.*, *25*, 1347–1350, doi:10.1029/97GL03226.

Di Girolamo, P., B. B. Demoz, and D. N. Whiteman (2003), Model simulations of melting hydrometeors: A new lidar bright band from melting frozen drops, *Geophys. Res. Lett.*, *30*(12), 1626, doi:10.1029/2002GL016825.

Fabry, F., and I. Zawadzki (1995), Long-term radar observations of the melting layer of precipitation and their interpretation, *J. Atmos. Sci.*, *52*, 838–851.

Fabry, F., G. L. Austin, and D. Tees (1992), The accuracy of rainfall estimates by radar as a function of range, *Q. J. R. Meteorol. Soc.*, *118*, 435–453.

Giangrande, S. E. (2007), Investigations of polarimetric measurements of rainfall at close and distant ranges, PhD dissertation, 203 pp., Univ. of Oklahoma, Norman, Okla.

Heymsfield, G. M., S. W. Bidwell, P. E. Racette, I. J. Caylor, S. Ameen, S. Nicholson, W. Boncyk, L. Miller, D. Vandemark, and L. R. Dod (1996), The EDOP radar system on the high-altitude NASA ER-2 aircraft, *J. Atmos. Oceanic Technol.*, *4*, 795–809.

Ikeda, K., E. A. Brandes, and R. M. Rasmussen (2005), Polarimetric radar observations of multiple freezing levels, *J. Atmos. Sci.*, *62*, 3624–3636.

Kummerow, C., W. Barnes, T. Kozu, J. Shuie, and J. Simpson (1998), The Tropical Rainfall Measuring Mission (TRMM) sensor package, *J. Atmos. Oceanic Technol.*, *15*, 809–817.

Marshall, J. S., R. C. Langille, and W. McK. Palmer (1947), Measurement of rainfall by radar, *J. Meteorol.*, *4*, 186–192.

Martner, B. E., J. B. Snider, R. J. Zamora, G. P. Byrd, T. A. Niziol, and P. I. Joe (1993), A remote-sensing view of a freezing rain storm, *Mon. Weather Rev.*, *121*, 2563–2577.

Martner, B. E., P. J. Neiman, and A. B. White (2007), Collocated radar and radiosonde observations of a double-brightband melting layer in Northern California, *Mon. Weather Rev.*, *135*, 2016–2024.

Marwitz, J. D. (1983), The kinematics of orographic airflow during Sierra storms, *J. Atmos. Sci.*, *40*, 174–185.

Marwitz, J. D. (1987), Deep orographic storms over the Sierra Nevada. Part I: Thermodynamic and kinematic structure, *J. Atmos. Sci.*, *44*, 159–172.

Melnikov, V. (2013), Wet ice cloud particles at subfreezing temperatures?, AMS Radar Meteorology Conference. Breckenridge, CO, Conference preprint.

Mitra, S. K., O. Vohl, M. Ahr, and H. R. Pruppacher (1990), A wind tunnel and theoretical study of the melting behavior of atmospheric ice particles. IV: Experiment and theory of snowflakes, *J. Atmos. Sci.*, *47*, 584–591.

Plank, V. G., D. Atlas, and W. H. Paulsen (1955), The nature and detectability of clouds and precipitation as determined by a 1.25 centimeter radar, *J. Meteorol.*, *12*, 358–370.

Pruppacher, H. R., and J. D. Klett (1978), *Microphysics of Clouds and Precipitation*, 714 pp., D. Reidel, Boston, Mass.

Sassen, K., and T. Chen (1995), The lidar dark band: An oddity of the radar bright band analogy, *Geophys. Res. Lett.*, *22*, 3505–3508, doi:10.1029/95GL03367.

Stewart, R. E., J. D. Marwitz, J. C. Pace, and R. E. Carbone (1984), Characteristics through the melting layer of stratiform clouds, *J. Atmos. Sci.*, *41*, 3227–3237.

White, A. B., D. J. Gottas, E. T. Storm, F. M. Ralph, and P. J. Neiman (2002), An automated brightband height detection algorithm for use with Doppler radar spectral moments, *J. Atmos. Oceanic Technol.*, *19*, 687–697.

Willis, P. T., and A. J. Heymsfield (1989), Structure of the melting layer in mesoscale convective system stratiform precipitation, *J. Atmos. Sci.*, *46*, 2008–2025.